THERMO-HYDRO-MECHANICAL COUPLING IN CLAY BARRIERS

F. Collin, X.L. Li, J.-P. Radu and R. Charlier,
MSM Department, University of Liege, Belgium,
Member of the ALERT GEOMATERIALS network

Abstract

A thermo-hydro-mechanical model is presented to tackle the complex coupling problems encountered in clay barriers. A detailed formulation coupling heat, moisture (liquid water and water vapour) and air transfer in a deformable unsaturated soil is given. The formulation of Alonso-Gens's mechanical model for unsaturated soil is also incorporated. The sensitivity to some parameters and their determinations are analysed. Finally, a small scale wetting – heating test on compacted bentonite is performed for validation; the numerical results are compared to the experimental measurements.

1. Introduction

Some nuclear waste disposal concepts are based on the waste storage in deep clay geological layers. The nuclear canisters are surrounded by highly compacted clay, which undergoes initially a very high suction (up to 100 MPa or more) and this suction modifies the hydro-mechanical behaviour. Moreover the confinement barrier is subject to high temperature (over 70°C and sometimes over 100°C). A good design of a clay barrier should take all these phenomena into account. For this purpose, constitutive laws have been developed. They are coupling water flow, heat flow and soil mechanic. They have been implemented in a finite element code, which allows analysing non-homogenous transient problems.

The mechanical behaviour of a unsaturated soil depends of stress level and of suction. A refined model has been proposed ten years ago by Alonso and Gens. On the other hand, the water flow in unsaturated media is a non-linear problem. Moreover high temperature induces the production of water vapour (which depends also on the suction level). Its modelling is based on Philip's and de Vries's contribution.

The developed finite elements are based on the following degrees of freedom: soil skeleton displacements, temperature, liquid water pressure, and gas (dry air + vapour) pressure. The elements have a monolithically form, and all coupling terms in the Newton-Raphson stiffness matrix are taken into account, allowing a good convergence rate for most treated problems.

A validation of the constitutive laws and of the finite element code is obtained thanks to a comparison with other code results and with some experimental results.

2. Diffusion model

In clay barriers, unsaturated conditions and thermal variations create several coupling effects that influence the design of each component of the barriers. Moreover high temperatures in unsaturated conditions induce production of water vapour. Thus, gas phase is a mixture of dry air and water vapour. Liquid water and dissolved air compound the liquid phase.

The variables chosen for the description of the flow problem are liquid water pressure, gas pressure and temperature.

2.1 Water species

The mass conservation equation is written for the mass of liquid water and water vapour. Vapour flows will have significant effects on moisture transfer only if liquid and vapour flows have a same order of magnitude.

Clay presents a very low permeability and very slow liquid water motions. So the effect of water vapour transport in this type of soil may not be neglected.

2.1.1 Mass conservation for the water

The equation includes the variation of water storage and the divergence of water flows, including the liquid and vapour effects:

$$\underbrace{\frac{\partial \rho_w n S_{r,w}}{\partial t} + div(\rho_w \underline{f}_w)}_{\text{Liquid water}} + \underbrace{\frac{\partial \rho_v n S_{r,g}}{\partial t} + div(\rho_v \underline{f}_v + \rho_v \underline{f}_g)}_{\text{Water vapour}} = 0 \qquad (2.1)$$

Where ρ_w is liquid water density; n is medium porosity; $S_{r,w}$ is water saturation degree in volume; $\underline{f}_\alpha$ is macroscopic velocity of the component α; ρ_v is water vapour density; $S_{r,g}$ is gas saturation degree in volume and t is the time.

Water vapour is one of the gas phase's compounds. Therefore, vapour flows thanks to vapour diffusion in the gaseous phase and to gas convection.

2.1.2 Motion of the liquid water

The generalised Darcy's law for multiphase porous medium gives liquid water velocity:

$$\underline{f}_w = -\frac{k_{int} k_{r,w}}{\mu_w}\left[\underline{\nabla} p_w + g \rho_w \underline{\nabla} y\right] \qquad (2.2)$$

Where p_w is the liquid water pressure; y is the vertical, upwards directed co-ordinate; g is the gravity acceleration; μ_w is the dynamic viscosity of the liquid water; k_{int} is the intrinsic permeability of the medium and $k_{r,w}$ is the water relative permeability.

The water permeability varies with respect to the saturation degree in unsaturated conditions.

2.1.3 Couplings between the liquid water and other variables

The liquid water properties (i.e. density and viscosity) depend on temperature. This induces a coupling between liquid water flow and thermal flow: some convective water flows can be created due to temperature distribution. Another coupling effect is due to permeability, which depends on suction (i.e. the difference between the gas and water pressure). The suction field will influence the water flows.

2.1.4 Diffusion of water vapour

The water vapour flow is assumed to follow a Fick's diffusion law. The vapour diffusion is due to a gradient of vapour density :

$$\underline{f}_v = -D\underline{\nabla}\rho_v \tag{2.3}$$

The water vapour density ρ_v is given by thermodynamic relations (Edlefsen & Anderson 1943):

$$\rho_v = \rho_0 h \tag{2.4}$$

Where ρ_0 is the saturated water vapour density and h is the relative humidity.

The Kelvin-Laplace's law gives the relative humidity h:

$$h = \exp\left(\frac{p_w - p_g}{\rho_w R_v T}\right) \tag{2.5}$$

Where R_v is the gas constant of water vapour and T is the temperature.

The relative humidity allows taking into account adsorption phenomena and capillary effect in the soil.

The diffusion coefficient D is not easy to determine. It is supposed to depend on the saturation degree and the tortuosity. Following Philip's and de Vries's model (Philip & de Vries 1957), the following relation is assumed:

$$D = \frac{D_{atm} \nu_v \tau_v n S_{r,g}}{\rho_v} \tag{2.6}$$

Where D_{atm} is the diffusion coefficient; ν_v is the 'mass flow' factor and τ_v is the tortuosity.

The vapour is considered as a perfect gas and the perfect gas law gives the vapour pressure:

$$p_v = \rho_v R_v T \tag{2.7}$$

The gradient of the water vapour density can now be developed in order to compute the vapour flow:

$$\underline{\nabla}\rho_v = \frac{\rho_0 g h}{R_v T}\underline{\nabla}\frac{p_w - p_g}{\rho_w g} + \left[h\frac{\partial \rho_0}{\partial T} - \frac{\rho_0\left(p_w - p_g\right)h}{\rho_w R_v T^2}\right]\underline{\nabla}T \tag{2.8}$$

The water vapour density gradient can be separated into two contributions: an isothermal one related to a suction gradient and a thermal one due to a temperature gradient.

2.1.5 Couplings between the water vapour and other variables

As shown above, the vapour properties and flows depend essentially on temperature and on gas pressure fields. This model can reproduce the vapour transport from the points at high temperature (where the water vapour is produced) to the points at lower temperature (where the water vapour condenses).

2.2 Dry air species

Dry air is a part of a gas mixture: dry air and water vapour compose the gas phase. But there is also dissolved air in the water that has to be taken into account. The dry air pressure is not a basic variable: this pressure will be computed up to the gas and the vapour pressure.

Dalton's law is assumed: the pressure of the gas mixture is equal to the sum of the partial pressures, which each gas would exert if it filled alone all the volume considered.

2.2.1 Mass conservation for the dry air

The equation of mass conservation includes the contributions of the dry air phase and of the dissolved air in water:

$$\underbrace{\frac{\partial \rho_a n S_{r,g}}{\partial t} + div(\rho_a \underline{f}_a + \rho_a \underline{f}_g)}_{\textit{Dry air in gas phase}} + \underbrace{\frac{\partial H \rho_a n S_{r,w}}{\partial t} + div(H\rho_a \underline{f}_w)}_{\textit{Dissolved air in water}} = 0 \tag{2.9}$$

Where ρ_a is dry air density and H is Henry's coefficient.

Henry's coefficient H allows determining the dissolved air in the liquid water. The dissolved air mass is supposed to be sufficiently low in order to consider that the water properties are not influenced. The dry air flow in the gaseous phase is due to the flow of the gas mixture and to the dry air diffusion flow.

2.2.2 Diffusion of dry air

The dry air diffusion flow is related to dry air density gradient. Using the diffusion theory adapted to porous medium, the diffusion dry air flows can be computed by :

$$\underline{f}_a = -\left[D_{atm}.\nu_v.\tau_v.\theta_g / \rho_a\right]\underline{grad}(\rho_a) \tag{2.10}$$

2.2.3 Motion of gas

The generalised Darcy's law for multiphase medium gives the gas velocity:

$$\underline{f}_g = -\frac{k_{int} k_{r,g}}{\mu_g}\left[\underline{\nabla} p_g + g\rho_g \underline{\nabla} y\right] \tag{2.11}$$

Where μ_g is the gas dynamic viscosity; $k_{r,g}$ is the gas relative permeability and ρ_g is the gas density.

The gas permeability is adapted in order to reproduce its variation in non-saturated conditions.

2.3 Heat diffusion

2.3.1 Conservation of the heat

$$\frac{\partial \phi}{\partial t} + div(\underline{q}) - Q = 0 \tag{2.12}$$

Where ϕ is the enthalpy of the medium; $\underline{q}$ is the heat flow and Q is a volume heat source.

2.3.2 Quantity of heat storage: Enthalpy

The enthalpy of the system is given by the sum of each component's enthalpy:

$$\begin{aligned}\phi = {} & nS_{r,w}\rho_w c_{p,w}(T - T_0) + nS_{r,g}\rho_a c_{p,a}(T - T_0) \\ & + (1-n)\rho_s c_{p,s}(T - T_0) + nS_{r,g}\rho_v c_{p,v}(T - T_0) \\ & + nS_{r,g}\rho_v L\end{aligned} \tag{2.13}$$

Where $c_{p,\alpha}$ is the specific heat of the component α and L is the vaporisation latent heat. The last enthalpy term corresponds to the heat stored during the water vaporisation.

2.3.3 Heat transport

The heat transport is related to the conduction effect, the convection one and the vaporisation one.

$$\begin{aligned}\underline{q} = {} & -\Gamma \underline{\nabla} T + \left[c_{p,w}\rho_w \underline{f}_w + c_{p,a}\rho_a(\underline{f}_a + \underline{f}_g) + c_{p,v}\rho_v(\underline{f}_v + \underline{f}_g)\right](T - T_0) \\ & + \left(\rho_v \underline{f}_v + \rho_v \underline{f}_g\right)L\end{aligned} \tag{2.14}$$

Where Γ is the medium conductivity.

Some authors explicitly model also the solid convection, which is typically a large strains, large displacements effect. Our model takes the large strains and large rotations of the sample into account, thanks to a Lagrangian actualised formulation. Therefore the equilibrium and balance equations, as well as the water, air, and heat flow are expressed in the moving current

configuration. This implies that the solid convection effect is implicitly taken into account.

2.3.4. Couplings

The principal coupling effect results from the convection: a quantity of heat is transported by water, vapour and air flow.

3. Mechanical behaviour modelling

Suction has a strong influence on the mechanical properties of soil: hardness and shear strength of soil increase with suction; swelling or collapse can be induced, even some irreversible deformations can take place... So, the mechanical behaviour modelling should be able to take these suction effects into account.

The application of the concept of *effective stress* to the mechanical behaviour modelling of an unsaturated soil has some limitations. Use of the *independent stresses state variables* to model the mechanical behaviour of unsaturated soils seems to be more and more convincible (Fredlund & Morgenstern 1977). That is:

$$\begin{aligned} &\text{the net stresses tensor : } \sigma_{ij}^{*} = \sigma_{ij} - p_g \delta_{ij} \\ &\text{the suction : } \qquad\qquad s = p_g - p_w \end{aligned} \tag{3.1}$$

3.1 Mechanical model

Alonso et al (Alonso et al. 1990) have proposed a mechanical model, which is written in the framework of the *independent stresses state variables*. It is based on the well-known CamClay model. In our finite element code *LAGAMINE*, the plastic yield surfaces are written in a three-dimensional stress space: $I_{\sigma}^{*} - II_{\hat{\sigma}}^{*} - s$ where I_{σ}^{*} is the first net stress invariant and $II_{\hat{\sigma}}^{*}$ refers to the second net deviatoric stress invariant.

$$I_{\sigma}^{*} = \sigma_{ii} \tag{3.2}$$

$$II_{\hat{\sigma}}^{*} = \sqrt{\frac{1}{2}\hat{\sigma}_{ij}\hat{\sigma}_{ij}} \tag{3.3}$$

At a given value of suction, the yield surface in the $I_{\sigma}^{*} - II_{\hat{\sigma}}^{*}$ space is written as:

$$F_1 = \left(I_{\sigma}^{*2} + (I_0 - P_s) I_{\sigma}^{*} - I_0 P_s \right) \bar{r}^2 + II_{\hat{\sigma}}^{*2} \tag{3.3}$$

Where $\bar{r}$ represents the critical state line of soil and depends on the Lode's angle. P_s characterises the resistance of soil on isotropic extension stress path and varies with the suction. I_0 refers to the pre-consolidation of soil and is a function of the suction (Fig. 3.1):

$$I_0 = p_c \left(\frac{I_0^{*}}{p_c} \right)^{\frac{\lambda(o)-\kappa}{\lambda(s)-\kappa}} \tag{3.4}$$

Where I_0^* represents the pre-consolidation pressure of soil in saturated condition. p_c is a reference pressure. $\lambda(s)$ refers to the plastic slope of the compressibility curve against the net mean stress, it varies with the suction followed by:

$$\lambda(s) = \lambda(0)\left[(1-r)exp(-\beta s) + r\right] \tag{3.5}$$

$\lambda(0)$ is the plastic slope for the saturated condition. The elastic slope κ of the compressibility curve against the net mean stress, may also be function of the suction. r and β are parameters.

The irreversible deformation upon drying can be modelled with the help of another yield surface (*SI*) in the $I_\sigma^* - s$ plan, (Fig. 3.1):

$$F_2 = s - s_0 \tag{3.6}$$

Where s_0 is a yield suction value which represents the maximum value of suction sustained by the soil.

The preconsolidation pressure curve in the $I_\sigma^* - s$ plan (equation 3.4) defines another part of the yield surface called LC (Loading Collapse) which serves for modelling the collapse behaviour under wetting.

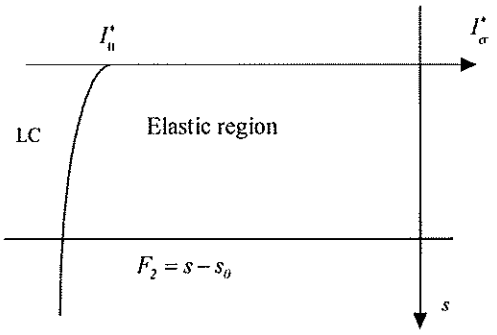

Figure 3.1. Yield surface in the plan $I_\sigma^* - s$

The model responses include principally three parts.
The strains induced by stress variations (mechanical solicitation) are given by:

$$\begin{aligned} \dot{\varepsilon}_{ij}^e &= C_{ijkl}^{e\ -1}\dot{\sigma}_{ij} \text{ (elastic deformations)} \\ \dot{\varepsilon}_{ij}^p &= \dot{\lambda}\frac{\partial G}{\partial \sigma_{ij}} \text{ (plastic deformations)} \end{aligned} \tag{3.7}$$

Where C_{ijkl}^e is the Hooke's tensor, G is the plastic potential surface, and $\dot{\lambda}$ is obtained from the consistency condition.

The deformations induced by suction evolution (hydric path) are:

$$\dot{\varepsilon}^{e}_{kl-s} = \frac{\kappa_s}{3(1+e)(s+P_{at})}\dot{s}\delta_{kl} \quad (\text{if } s < s_0)$$
$$\dot{\varepsilon}^{p}_{kl-s} = \frac{\lambda_s - \kappa_s}{3(1+e)(s+P_{at})}\dot{s}\delta_{kl} \quad (\text{if } s \geq s_0) \tag{3.8}$$

Where λ_s and κ_s are the stiffness parameters for changes in suction and P_{at} is atmospheric pressure. It should be noted that λ_s and κ_s could vary with the stress level.

The elastic thermal dilatation of soil is introduced in the model by:

$$\dot{\varepsilon}^{e}_{kl-T} = \alpha\dot{T}\delta_{kl} \tag{3.9}$$

Where α is the dilatation coefficient of soil.

The yield surface evolution is controlled by the total plastic volumetric strain ε_v^p developed in the soil via two state variables I_0^* and s_0.

4. Validation test

The following modelling has been performed in the framework of a European Community research project entitled *Calculation and testing of behaviour of unsaturated clay (Catsius clay)*, to investigate both temperature and artificial hydration effects on the deformation and moisture transfer in the soil. The results of a small-scale wetting-heating test performed on highly compacted bentonite have been available. The test has been performed inside a thermohydraulic cell, which is schematised in figure 4.1. The sample has been heated by means of the central heater and hydrated through the ports that are connected to the porous plate. During the test, the temperatures at different points, the volume of water flow and the swelling pressures generated in one point of the sample have been measured. The outer cell surface has been in contact with ambient air. The experience has elapsed during 2401.6 hours.

A finite element simulation is realised with the help of the developed finite elements with five-freedom degrees. The heating is modelled by imposing the temperature on the nodes of the sample in contact with the heater. The hydration procedure is modelled by increasing the water pressure on the nodes of porous plate. The convection transfer between the steel case and the ambient atmosphere is modelled thanks to the frontier thermal elements.

The steel case is supposed to be impermeable to the water flow. Both steel case and porous plate deformations are neglected. The system is initially at ambient temperature (293 °K). The gas pressure is supposed to remain fixed to the atmospheric pressure (100 kPa). The initial saturation of soil is 49% which gives an initial suction s =78.6 MPa according to the water retention curve.

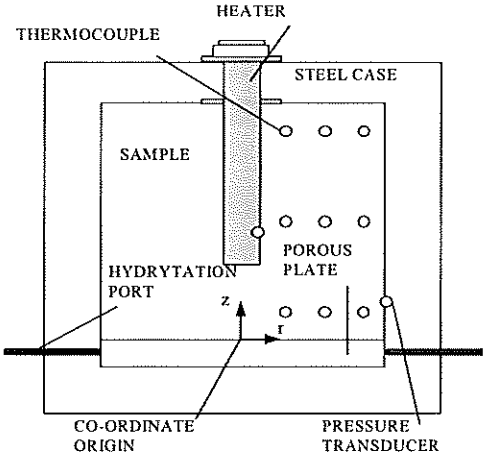

Fig. 4.1 Configuration of the thermohydraulic cell

4.1 Hydraulic and thermal properties

An equation describing the water retention curve is chosen to reproduce the measured data:

$$S_{r,w} = S_{r,res} + CSW3\frac{(S_{r,field} - S_{r,res})}{CSW3 + (CSW1.s)^{CSW2}} \tag{4.1}$$

Where $S_{r,field}$ is the maximum saturation in the soil and $S_{r,res}$ is the residual saturation for a very high value of suction.

The water relative permeability is determined by:

$$k_{r,w} = \frac{(S_{r,w} - S_{r,res})^{CKW}}{(S_{r,field} - S_{r,res})^{CKW}} \text{ if } S_{r,w} \geq S_{r,res}$$
$$k_{r,w} = k_{r,w,min} \qquad \text{if } S_{r,w} < S_{r,res} \tag{4.2}$$

The gas relative permeability is modelled by:

$$k_{r,g} = (1 - S_e)^{CKA1}.(1 - S_e^{CKA2}) \tag{4.3}$$

Where S_e the effective saturation.

The water retention curve and the permeability are found to have an important influence on the water intake volume and the final saturation degree. The soil conductivity is a function of the saturation degree.

4.2 Parameters related to the mechanical model

The results of two series of suction controlled oedometer tests have been obtained to get the mechanical parameters. First one includes some tests with wetting-drying cycles under

different constant vertical pressures. Another series of tests has been realised following several loading-unloading cycles under different constant suctions. By this way, the suction yield parameter s_0 is obtained by the water retention curve.

4.3 Comparisons between simulation and experimental results

The figure 4.2 shows water intake evolution with time. A very good result is obtained: the experimental and numerical curves are almost the same.

The figure 4.3 shows the comparison between experimental and numerical result of the swelling pressure at the point with co-ordinates r=7.5 cm and z=1.25 cm during the experience. The agreement is good at the beginning, but decreases at the end of experience. In fact, the model didn't take into account some variations of certain parameters for this simulation, like κ_s varying with the net stress, κ depending on the suction, etc…

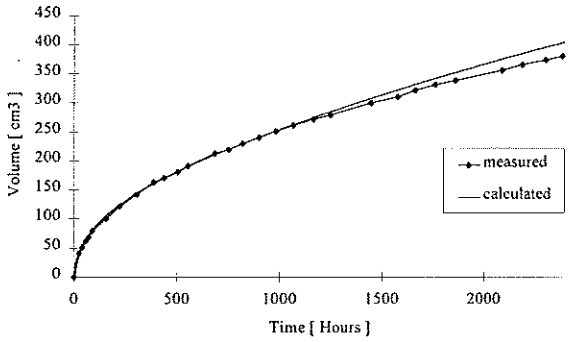

Fig. 4.2 Water intake evolution

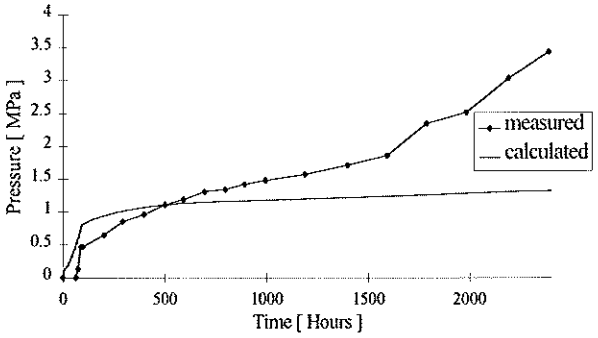

Fig. 4.3 Swelling pressure evolution

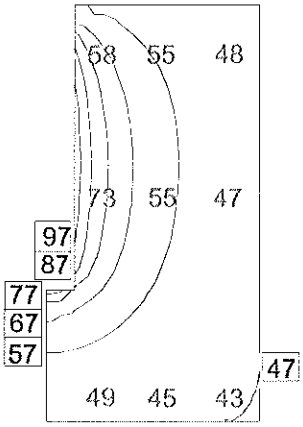

Fig.4.4 Temperature field at the end of experience

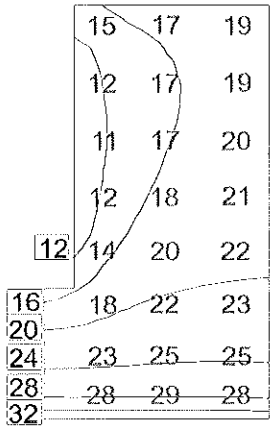

Fig. 4.5 Water content at the end of experience

The calculated temperatures and water contents at the end of the experience are given in figure 4.4 and 4.5 respectively. The corresponding experimental measurements at some points are also presented in grey on the same figure. The calculated temperatures are a little higher than the experimental ones. The numerical water content seems to be slightly lower than the experimental one at the analysed points. But they are close to the experimental ones near the heater. The generation of water vapour near the heater is a crucial phenomenon to take here in account. The vapour flow depends deeply on the temperature.

All the results appear to be very sensitive to the retention curve, the relative and intrinsic permeability.

A last remark could be that the soil mechanics has not a high influence on the water flow. Oppositely, the water flow has a deep influence on the mechanical behaviour.

4.4 Influence of the gas pressure

In the previous simulation, the gas pressure remains fixed to the atmospheric pressure. The (constant or variable) gas pressure effect has been checked thanks to simulations performed with (Case A) and without (Case B) a fixed gas pressure. In the case B, the steel case is supposed impermeable to gas. For both cases, the mechanical model is not taken into account.

On the following pictures, the left part is the results of the case A and the right part of the case B.

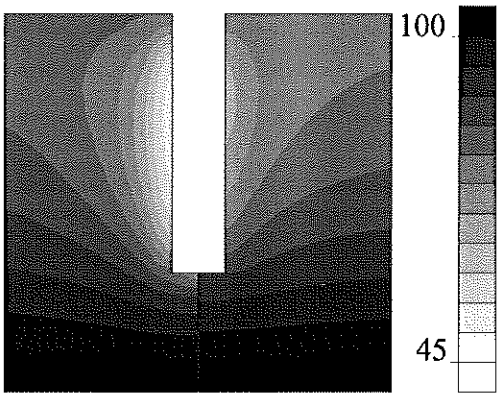

Fig. 4.6 Saturation (%)
at the end of the experiment

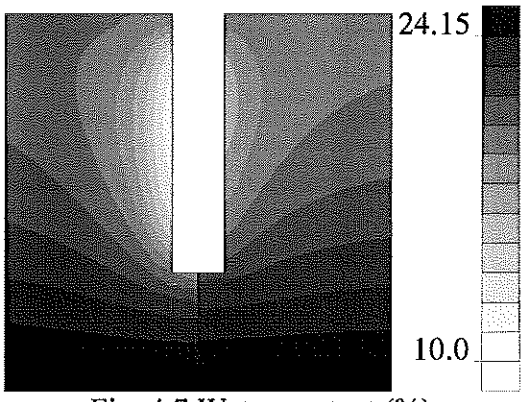

Fig. 4.7 Water content (%)
at the end of the experiment

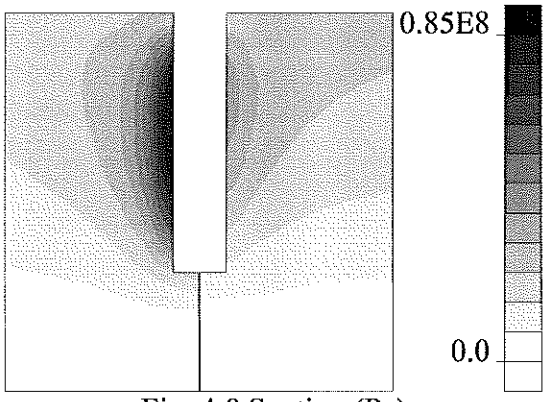

Fig. 4.8 Suction (Pa)
at the end of the experiment

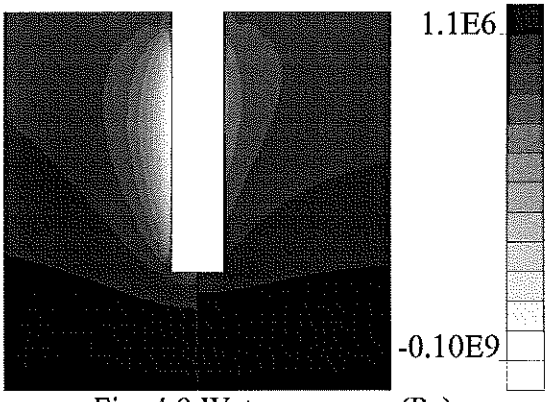

Fig. 4.9 Water pressure (Pa)
at the end of the experiment

The results show clearly differences between the two simulations. The saturation degree in case A varies from 47% to 100% while it varies from 62% to 100% in case B. In terms of suction, it means that the sample is submitted to a maximum suction of 85.1 MPa in case A and of 40.3 MPa in case B.

The computations have also shown that the gas pressure increases in a range from 302 kPa to 463 kPa.

This gas pressure increase should also have an influence on mechanical behaviour. Indeed, this increase modifies suction field and net stresses, which are the *independent variables* of the mechanical model.

5. CONCLUSION

A complete theory of a thermo-hydro-mechanical coupling model for unsaturated soils is provided in this paper. A validation test is performed to show the capabilities of the model to simulate the relevant phenomenon in nuclear energy storage. The comparison between simulation results and experimental ones is discussed. Some sensitivity of the mechanical parameters is also mentioned.

Acknowledgements

The authors thank the Europe Community for the support through the research project *Catsius clay* project. The support from FNRS is also greatly acknowledged.

References

Alonso, E.E. & Gens, A. & Josa, A.A. (1990). "A constitutive model for partly saturated soil". *Géotechnique*. **40**, n°3: 405-430.

Edlefsen, N. E. & Anderson, A.B.C. (1943). "Thermodynamics of soils moisture". *Hilgardia*. **15**, No. 2: 31-298.

Fredlund, D.G. & Morgenstern, N.R. (1977). "Stress state variables for unsaturated soils". *J. Geotech. Eng. Div. A.S.C.E.* **103** GT5: 447-466.

Philip, J.R. & de Vries, D.A. (1957). "Moisture movement in porous materials under temperature gradients". *Trans. Am. Geophys. Un.* **38**: 222-232.